

Efimov states embedded in the three-body continuum

N. P. Mehta,^{*} Seth T. Rittenhouse,[†] J. P. D’Incao,[‡] and Chris H. Greene[§]
Department of Physics and JILA, University of Colorado, Boulder, CO 80309-0440
 (Dated: February 9, 2022)

We consider a multichannel generalization of the Fermi pseudopotential to model low-energy atom-atom interactions near a magnetically tunable Feshbach resonance, and calculate the adiabatic hyperspherical potential curves for a system of three such interacting atoms. In particular, our model suggests the existence of a series of quasi-bound Efimov states attached to excited three-body thresholds, far above open channel collision energies. We discuss the conditions under which such states may be supported, and identify which interaction parameters limit the lifetime of these states. We speculate that it may be possible to observe these states using spectroscopic methods, perhaps allowing for the measurement of multiple Efimov resonances for the first time.

Three resonantly interacting particles may form long-range bound states, called Efimov states [1], even if the short-range interparticle interaction supports no two-body bound states. After years of tantalizing work on atomic ^4He trimers and halo nuclei (see [2] and references therein), the first strong experimental evidence of Efimov physics was recently found in an ultracold thermal gas of cesium atoms [3]. This observation was made possible by utilizing a magnetically tunable Feshbach resonance to precisely control the two-body scattering length over a substantial range, and observing a resonant feature in the atom-loss rate due to three-body recombination [4, 5, 6]. Since hyperspherical studies have provided important insights in the past [5, 7, 8], we are motivated in this Letter to investigate the nature of universality within the adiabatic hyperspherical representation for multichannel two-body interactions, obtaining a complete view of the complicated energy landscape.

Multichannel systems have a considerably richer structure than their single-channel counterparts [9], admitting multiple three-body thresholds, quasi-bound two-body channels, and multiple length scales. In this Letter, we present a Green’s function method for obtaining the adiabatic potential curves, and discuss some immediate consequences. Note that the zero-range multichannel method developed initially by Macek and Kartavtsev to study three-body recombination near a narrow two-body Feshbach resonance [11] is the closest existing study to the present analysis, but it did not consider our main point of focus, namely the Efimov effect for *excited* three-body thresholds.

Efimov states attached to *excited* three-body thresholds are absent in single channel models and difficult to infer from other multichannel approaches [12]. For these excited thresholds, at least one of the three atoms resides in an excited Zeeman or hyperfine state. We label these one-atom states $|1\rangle$ and $|2\rangle$ with energies $E_1 = 0$ and $E_2 = \epsilon$, respectively. In particular, we show that under the rather general stipulation that a quasibound two-body state is degenerate with an excited two-body threshold (see Fig. 1), and that the coupling between product states $|11\rangle$ and $|22\rangle$ is much smaller than all other

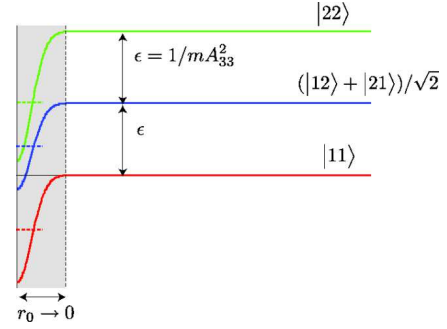


FIG. 1: (color online) A schematic representation of our two-body model is shown. As the range r_0 is taken to zero, the potential is regularized by the derivative in Eq. (1)

couplings, a series of Efimov states should emerge that is attached to an excited three-body threshold. These Efimov states are of a unique character and can be viewed as fully three-body Fano-Feshbach resonances embedded within the three-body continuum far above the energy of open channel collisions, in contrast with the single-channel Efimov resonances predicted and recently observed that were interpreted as shape resonances [4, 5]. Since the interatomic scattering length for ground-state atoms will not in general be resonant, the gas will be comparatively stable with respect to the a^4 scaling law for three-body recombination [2, 4, 5]. Efimov states attached to the excited threshold could be directly accessed via photoassociation and observed through the measurement of atom-loss rates, thus opening a new toolkit of powerful spectroscopic techniques [14].

As illustrated in Fig. 1, the two-body system has a set of product states $\{|\sigma = 1\rangle, |\sigma = 2\rangle, |\sigma = 3\rangle\} = \{|11\rangle, (|12\rangle + |21\rangle)/\sqrt{2}, |22\rangle\}$ with respective energies $\{E_\sigma\} = \{0, \epsilon, 2\epsilon\}$. The zero-range two-body potential is now written in the $\{|\sigma\rangle\}$ basis as,

$$V(r) = \frac{4\pi A}{m} \frac{\delta(r)}{r^2} \frac{\partial}{\partial r}(r \cdot), \quad (1)$$

This potential is the natural extension of the regularized Fermi pseudopotential which imposes the Bethe-

Peierls boundary condition on the two-body wavefunction, $\psi(r) \rightarrow C(1 - a/r)$ as $r \rightarrow 0$. When all channels are energetically open, the matrix \underline{A} is simply minus the scaled two-body reaction matrix \underline{K}_0 . The physical reaction matrix is obtained from the multichannel quantum defect theory (MQDT) channel closing formula [15, 16]. Note that unlike other multichannel treatments that retain only one open background channel and a one resonant molecule channel [12], we label our channels explicitly by the internal states of the atoms, and our Hamiltonian allows for scattering at excited thresholds between atoms with different internal states.

Unless explicitly stated, we choose the energy independent symmetric matrix to have elements A_{ij} such that $A_{13} \rightarrow 0$, and $A_{33} = A_{11} \sim 3.75 a_0$ giving $\epsilon/h = \hbar^2/(hmA_{33}^2) \sim 3$ GHz and placing a quasi-bound state at $E = \epsilon$. The quantity A_{33} is the length scale by which we measure all other quantities for the remainder of this Letter. We choose $A_{12} = A_{23} = A_{33}/4$ to give a reasonable resonance width $\Delta_B \sim -8$ G, and $A_{22} = 2A_{33}$ in order to illustrate the effect of a quasi-bound two-body state on the three-body potential energy curves. These numbers are chosen to loosely model the 155 G resonance in ^{85}Rb . Explicitly allowing $A_{23} \neq A_{12}$ gives qualitatively similar results in the three-body calculations described below. Allowing $A_{13} \neq 0$ provides a direct coupling between $|11\rangle$ and $|22\rangle$ states and, as we discuss later, this coupling element is expected to limit the lifetime of Efimov states near $E = \epsilon$. We note that the methods of [15] permit the application of these ideas over a wider energy range because they include the long range van der Waals physics in the QDT treatment explicitly.

In the three-body system, we transform the mass-scaled Jacobi coordinates: $\vec{y}_1^{(i)} = (\vec{r}_j - \vec{r}_k)/d$ and $\vec{y}_2^{(i)} = d(\frac{\vec{r}_i + \vec{r}_k}{2} - \vec{r}_j)$ (with $d = 2^{1/2}/3^{1/4}$) into hyperspherical coordinates by defining the hyperangle α as $\tan \alpha^{(i)} = |y_1^{(j)}|/|y_1^{(k)}|$, the hyperradius R as $R^2 = \vec{y}_1^2 + \vec{y}_2^2$ (which is invariant under permutations) and the spherical polar angles $\omega_i = \{\theta_i, \phi_i\}$ point in the direction of \vec{y}_i . The angular coordinates $\{\alpha, \omega_1, \omega_2\}$ are collectively denoted Ω . The pair-wise interactions are written in the basis of two-body internal states, with the third spectator particle (near any chosen two-particle coalescence point) in either $|1\rangle$ or $|2\rangle$. Hence, if particle 1 is the spectator particle, the basis of internal states is $\{|\Sigma\rangle\} = \{|111\rangle, (|112\rangle + |121\rangle)/\sqrt{2}, |211\rangle, |122\rangle, (|212\rangle + |221\rangle)/\sqrt{2}, |222\rangle\}$ with energies $\{E_\Sigma\} = \{0, \epsilon, \epsilon, 2\epsilon, 2\epsilon, 3\epsilon\}$.

In the multichannel generalization [11] of the adiabatic hyperspherical method [17], we seek solutions to:

$$\left(\frac{\Lambda^2}{2\mu R^2} + \underline{E}_{th} + \underline{V}(R, \Omega) \right) \vec{\Phi}(R; \Omega) = U(R) \vec{\Phi}(R; \Omega) \quad (2)$$

Here, \underline{E}_{th} is a diagonal matrix $[E_{th}]_{\Sigma\Sigma'} = \delta_{\Sigma\Sigma'} E_\Sigma$, and $\underline{V}(R, \Omega)$ is the sum of matrices for each pair-wise interaction expressed in the basis $\{|\Sigma\rangle\}$. The three-body re-

duced mass is $\mu = m/\sqrt{3}$. The adiabatic potential is written in terms of the eigenvalue $\nu = \nu_1$ as $U(R) = \nu_1(\nu_1 + 4)/2\mu R^2$, where $\nu_\Sigma(\nu_\Sigma + 4) = 2\mu R^2(U(R) - E_\Sigma)$. Components of the free-space (diagonal) hyperangular Green's function $\underline{G}(\Omega, \Omega')$ satisfy,

$$(\Lambda^2 - \nu_\Sigma(\nu_\Sigma + 4)) G_{\Sigma\Sigma}(\Omega, \Omega') = \delta(\Omega, \Omega') \quad (3)$$

Defining $g_{l_1 l_2}^{\nu_\Sigma}(\alpha, \alpha') = N_{\nu_\Sigma l_1 l_2} f_{\nu_\Sigma l_1 l_2}^{(-)}(\alpha_{<}) f_{\nu_\Sigma l_1 l_2}^{(+)}(\alpha_{>})$, the most useful solution is written in the Sturm-Liouville form [18],

$$G_{\Sigma\Sigma}(\Omega, \Omega') = \sum_{l_1, m_1, l_2, m_2} [g_{l_1 l_2}^{\nu_\Sigma}(\alpha, \alpha') \times Y_{l_1 m_1}(\omega_1) Y_{l_1 m_1}^*(\omega'_1) Y_{l_2 m_2}(\omega_2) Y_{l_2 m_2}^*(\omega'_2)] \quad (4)$$

where f^- (f^+) is a solution to the homogeneous version of Eq. (3) regular at $\alpha = 0$ ($\alpha = \pi/2$), and the normalization $N_{\nu_\Sigma l_1 l_2}$ is fixed by the Wronskian of f^- and f^+ [19]. The hyperangular Lippmann-Schwinger (L-S) equation,

$$\Phi_\Sigma(\Omega) = -2\mu R^2 \sum_{\Sigma', k} \int d\Omega' G_{\Sigma\Sigma'}(\Omega, \Omega') V_{\Sigma\Sigma'}^{(k)}(R, \Omega') \Phi_{\Sigma'}(\Omega') \quad (5)$$

is then solved by evaluating the integral over $V_{\Sigma\Sigma'}^{(k)}$ in the coordinate system where $|\vec{y}_1^{(k)}| \propto |\vec{r}_i - \vec{r}_j| \propto R \sin \alpha^{(k)}$. The zero-range s-wave interaction immediately gives $l_1 = 0$, and $l_2 = L$. For this Letter, we confine our study to states with total orbital angular momentum $L = 0$. For equal-mass particles, in the limit $\alpha^{(k)} \rightarrow 0$ we have $\alpha^{(i)} = \alpha^{(j)} = \pi/3$; the L-S equation reduces to a matrix equation of the form [11]:

$$\left(\frac{3^{1/4}}{2^{1/2} R} \left(\underline{M}^{(1)} + \underline{M}^{(2)} \underline{P}_- + \underline{M}^{(3)} \underline{P}_+ \right) - \underline{1} \right) \vec{C}^{(1)} = 0 \quad (6)$$

where, for bosons,

$$M_{\Sigma\Sigma'}^{(i)} = \begin{cases} A_{\Sigma\Sigma'}^{(i)} \lambda_\Sigma \cot(\lambda_\Sigma \pi/2) & i = 1 \\ A_{\Sigma\Sigma'}^{(i)} \frac{-4 \sin(\lambda_\Sigma \pi/6)}{\sqrt{3} \sin(\lambda_\Sigma \pi/2)} & i = 2, 3 \end{cases} \quad (7)$$

The vector associated with the n^{th} eigenstate, $\vec{C}_n^{(1)}$ in Eq. (6), is defined by the boundary and normalization conditions:

$$C_{\Sigma, n}^{(k)} = \lim_{r_k \rightarrow 0} \frac{\partial(r_k \Phi_{\Sigma, n})}{\partial r_k} \quad \text{and} \quad \sum_{\Sigma} \langle \Phi_{\Sigma, n} | \Phi_{\Sigma, n} \rangle = 1. \quad (8)$$

We have rewritten the eigenvalue as $\nu_\Sigma = \lambda_\Sigma - 2$ purely for convenience, and \underline{P}_+ and \underline{P}_- perform cyclic and anticyclic permutations respectively upon the basis $\{|\Sigma\rangle\}$. Zeros of the determinant of the matrix in Eq. (6) yield the eigenvalues $\lambda_{\Sigma, n}^2 = 2\mu R^2(U_n(R) - E_\Sigma) + 1/4$. The potentials $U_n(R)$ appear in radial equations of the form (ignoring nonadiabatic effects): $-F_n''(R)/2\mu R^2 + U_n(R)F_n(R) = EF_n(R)$.

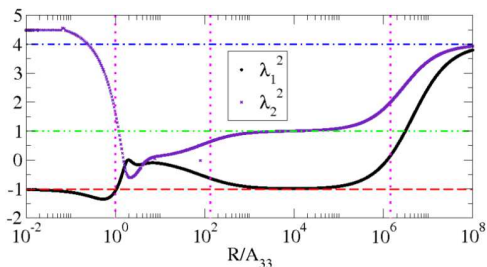


FIG. 2: (color online) The adiabatic eigenvalues λ_1^2 (λ_2^2) with respect to the first (second) threshold are shown for a near-resonant choice of ϵ . From left to right, the vertical dotted magenta lines mark A_{33} , $r_e = 132.284A_{33}$, and $a_{open} = -1.445 \times 10^6 A_{33}$. The horizontal dashed red line corresponds to the universal eigenvalue for three equal-mass resonantly interacting bosons $\lambda_1^2 = -1.012514$ [1], while the green dash-dot-dot line indicates the universal eigenvalue for only one resonant interaction $\lambda^2 = 1$, and the horizontal dash-dot blue line marks the lowest large R free-space eigenvalue $\lambda^2 = 4$.

In Fig. 2, we show eigenvalues with respect to the $E = 0$ and $E = \epsilon$ thresholds for ϵ chosen so that a quasi-bound two-body state is nearly degenerate with the $E = 0$ threshold, giving an identical boson (open-channel) scattering length of $a_{open} = -1.445 \times 10^6 A_{33}$. Note that we now drop the index n from the label of λ since the curves shown in Fig. 2 are actually comprised of many distinct eigenvalues connected by a series of close avoided crossings. This figure illustrates how the multichannel problem naturally introduces different length scales and symmetry constraints to the three-body problem. The eigenvalues may be understood by considering simultaneously the internal states of the atoms and the important natural length scales: A_{33} , the open-channel effective range r_e , and the open-channel scattering length a_{open} . When $R \ll A_{33}$, all length scales in our model appear long, so with respect to the lowest threshold, we have $\lambda_1^2 \rightarrow -1.012515$ appropriate for three resonantly interacting bosons. The region $A_{33} \ll R \ll r_e$ is a transitional regime indicating the importance of the r_e length-scale. In the region $r_e \ll R \ll |a_{open}|$, the potential near $E = 0$ behaves again as that of three resonantly interacting bosons, while near the second threshold $E = \epsilon$, only one of the interactions appears resonant and we obtain the appropriate value $\lambda_2^2 = 1$ [13]. For $|a_{open}| \ll R$, the eigenvalues approach the free-space value $\lambda_1^2 = \lambda_2^2 = 4$. Note that for values of R where $\lambda_1^2 < 0$ ($\lambda_2^2 < 0$) and is approximately constant, the potential with respect to the $E = 0$ ($E = \epsilon$) threshold is supercritical and supports Efimov states.

As mentioned before, by considering ϵ to vary with the magnetic field, it is possible to make a two-body state degenerate with the $|\sigma = 2\rangle$ threshold. This occurs when $\epsilon \rightarrow 1/(mA_{33}^2)$ as illustrated in Fig. 1. Provided that $|A_{13}| \ll A_{33}$, an Efimov potential appears at

both the $E = \epsilon$ and $E = 2\epsilon$ thresholds under these conditions. In Fig. 3(a) we show the lowest 300 adiabatic potential curves up to 3.5ϵ . Note the collection of three-body curves converging to each three-body threshold at $E = E_\Sigma$. Note also the quasi-bound two-body threshold near 0.6ϵ . A three-body collision near this energy will couple strongly to the two-body Feshbach resonance through this series of avoided crossings. In Fig. 3(c), the eigenvalue $\lambda_2^2 = \lambda_1^2 - 2\mu R^2\epsilon$ is shown to converge to the universal value $\lambda_2^2 = -0.171145$ predicted by the purely imaginary root of the corresponding single channel equation in the limit $|a| \rightarrow \infty$ [20] appropriate for two identical bosons interacting resonantly with a third distinguishable particle of equal mass, consistent with the fact that the $E = \epsilon$ threshold corresponds to internal states of the form $|\Sigma = 2\rangle = (|112\rangle - |121\rangle)/\sqrt{2}$ and $|\Sigma = 3\rangle = |211\rangle$. The spacing of Efimov states obeys the formula $E_n = E_0 \exp(-2\pi n/s_0)$, where $\lambda^2 \rightarrow -s_0^2$ in the universal regime, and E_0 is the energy of the lowest Efimov state. If we simply consider the value of the Efimov potential at $R \sim 100A_{33}$ to be a reasonable estimate for the energy of the first Efimov state, we obtain $E_0/h \sim (\epsilon/h) - (10\text{kHz})$. This places the second state at approximately $E_2/h \sim (\epsilon/h) - (1\text{mHz})$, giving a separation of roughly 10 kHz, within the resolution of modern radio-frequency experiments [14]. The spacing between states could be made more favorable by using heteronuclear mixtures of atoms, capitalizing on mass-ratios different from unity. [1, 20, 21].

In order for the Efimov states to persist at long-range, it is also necessary to show that the positive-definite non-adiabatic diagonal coupling $-Q(R) = -\langle \Phi(R) | \frac{\partial^2}{\partial R^2} | \Phi(R) \rangle$ corresponding to the Efimov potential falls off faster than R^{-2} . This is a non-trivial task since the potential is comprised of all potential curves approaching the lowest three-body threshold. We derive an expression for $-Q(R)$ [18] via a multichannel generalization of the method used in [10]. Our calculations indicate that the vector $\vec{C}^{(1)}$ (normalized according to Eq. (8)) for the eigenvalue corresponding to the Efimov potential has a dominant component: $C_{\Sigma=4}^{(1)}$, which grows linearly with R . Extrapolating this behavior for $\vec{C}^{(1)}$ and using the fact that $\lambda_2^2 \rightarrow -0.171145$ as R^{-1} , the expression for $-Q(R)$ reduces to the simple form: $-Q(R) = 3^{3/4} \sqrt{2} \pi^2 \frac{A_{33}^2 K_4}{R^3}$, where K_4 is the slope of the linearly increasing component $C_4^{(1)}$. Since $-Q(R)$ falls off faster than R^{-2} , we expect these states to persist at long range.

The lifetime of Efimov trimers near $E = \epsilon$ is limited by inelastic processes at short and long range. Using a WKB estimate, if all inelastic transitions occur at short range with probability P_{SR} (a reasonable assumption in the limit $A_{13} \rightarrow 0$), then the width of successive resonances will scale geometrically with the n^{th} energy level as $\Gamma_{SR} \approx P_{SR} E_0 e^{-2n\pi/s_0/s_0}$.

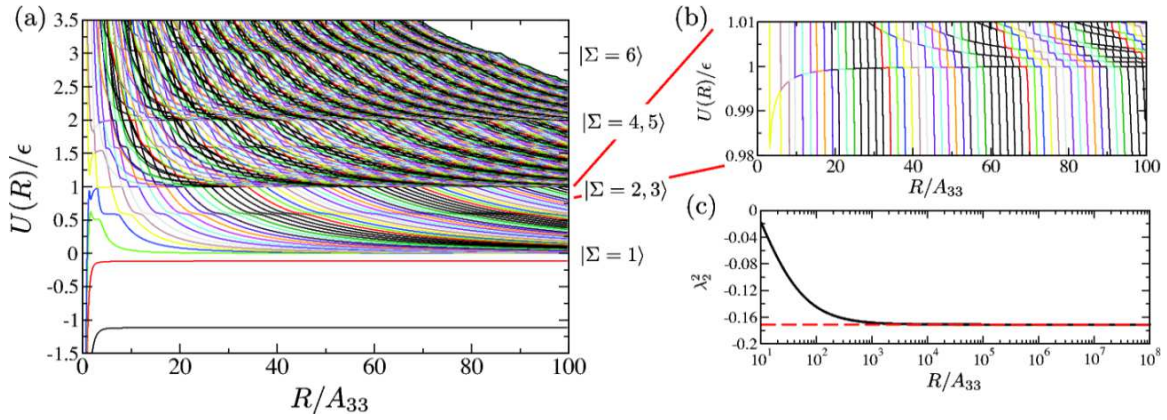


FIG. 3: In (a), we show approximately the lowest 300 potential curves up to 3.5ϵ , while (b) shows an enlarged view of the region near the $E = \epsilon$ threshold, and the attractive R^{-2} diabatic Efimov potential. Note also the series of avoided crossings in (a) near $E = 0.6\epsilon$ indicating the presence of a two-body quasi-bound state. In (c) we show the eigenvalue near $E = \epsilon$ converging to the universal value for two identical bosons and one distinguishable particle $\lambda^2 \rightarrow -0.171145$ indicated by the dashed red line.

For finite A_{13} inelastic transitions can also occur at long range due to two-body inelastic transitions, and the width of Efimov resonances is dominated by the size of A_{13} . Letting $A_{13} \neq 0$ serves to broaden the avoided crossing comprising the universal Efimov potential in Fig. 3(b), dramatically increasing the decay rate to three-body continuum states associated with the $|\Sigma = 1\rangle$ state, and making the Efimov states shorter lived and more difficult to observe. This is understood by noting that when the coupling between $|\sigma = 3\rangle$ and $|\sigma = 1\rangle$ is significant (i.e. A_{13} is sizable), direct inelastic transitions between $|\sigma = 3\rangle$ and $|\sigma = 1\rangle$ states dominate over inelastic transitions via the intermediate $|\sigma = 2\rangle$ state.

To summarize, we have identified a new class of Efimov states embedded in the three-body continuum. The hyperradial potentials supporting these states have universal properties consistent with the symmetry constraints implied by the internal degrees of freedom of the three-atom system, and can further be understood in terms of relevant two-body length scales. Further, we have identified the coupling constant A_{13} responsible for limiting the lifetime of these Efimov states at long range, and have shown that the repulsive diagonal nonadiabatic correction falls off as R^{-3} , consistent with the single-channel result. We stress that since the potential supporting these states appears when a quasi-bound two-body state is degenerate with an *excited* two-body threshold, the open-channel scattering length in general will not be resonant, and the gas is expected to be stable with respect to the a^4 recombination scaling law. We postulate that it may be possible to observe these states by spectroscopic techniques, perhaps with sufficient accuracy to measure two Efimov resonances for the first time.

We thank D. Blume and J. H. Macek for useful discussions during the early stages of this work. This work is supported by the National Science Foundation.

* mehtan@jilau1.colorado.edu

† rittenho@colorado.edu

‡ jpdincao@jilau1.colorado.edu

§ chris.greene@colorado.edu

- [1] V. Efimov, Sov. J. Nuc. Phys. **10**, 62 (1970).
- [2] E. Braaten and H.-W. Hammer, Phys. Rep. **428**, 259 (2006).
- [3] T. Kraemer *et al.*, Nature **440**, 315 (2006).
- [4] E. Nielsen and J. H. Macek, Phys. Rev. Lett. **83**, 1566 (1999).
- [5] B. D. Esry *et al.*, Phys. Rev. Lett. **83**, 1751 (1999).
- [6] E. Braaten and H.-W. Hammer, Phys. Rev. Lett. **87**, 160407 (2001).
- [7] J. P. D’Incao and B. D. Esry, Phys. Rev. Lett. **94**, 213201 (2005).
- [8] E. Nielsen *et al.*, Phys. Rep. **347**, 373 (2001).
- [9] A. Bulgac and V. Efimov, Sov. J. Nucl. Phys. **22**, 153 (1976).
- [10] O. I. Kartavtsev and A. V. Malykh, Phys. Rev. A. **74**, 042506 (2006); J. Phys. B. **40**, 1429 (2007).
- [11] O. I. Kartavtsev and J. H. Macek, Few Body Syst. **31**, 249 (2002); *ibid.* J. H. Macek, **31**, 241 (2002).
- [12] M. D. Lee *et al.*, Phys. Rev. A. **76**, 012720 (2007).
- [13] J. P. D’Incao and B. D. Esry, arXiv:0711.3238, (2007)
- [14] J. Léonard *et al.*, Phys. Rev. Lett **91**, 073203, (2003); C. A. Regal *et al.*, Nature **424**, 47 (2003); S. Gupta *et al.*, Science **300**, 1723 (2003); M. Bartenstein *et al.*, Phys. Rev. Lett. **94**, 103201 (2005).
- [15] J. P. Burke Jr. *et al.*, Phys. Rev. Lett **81**, 3355 (1998).
- [16] M. H. Ross and G. L. Shaw, Ann. Phys. **13**, 147 (1961).
- [17] J. H. Macek, J. Phys. B **1**, 831 (1968).
- [18] N. P. Mehta, S. T. Rittenhouse, and C. H. Greene (unpublished).
- [19] J. D. Jackson, *Classical Electrodynamics* (John Wiley and Sons, New York, 1999).
- [20] V. Efimov, Nucl. Phys. A. **210**, 157 (1973).
- [21] J. P. D’Incao and B. D. Esry, Phys. Rev. A. **73**, 030703(R) (2006).